JVI Journals.ASM.org

The Dominant-Negative Inhibition of Double-Stranded RNA-Dependent Protein Kinase PKR Increases the Efficacy of Rift Valley Fever Virus MP-12 Vaccine

Olga Lihoradova,[a] Birte Kalveram,[a] Sabarish V. Indran,[a] Nandadeva Lokugamage,[a] Terry L. Juelich,[a,e] Terence E. Hill,[b] Chien-Te K. Tseng,[b,c,d] Bin Gong,[a,d,e] Shuetsu Fukushi,[f] Shigeru Morikawa,[f] Alexander N. Freiberg,[a,c,d,e] and Tetsuro Ikegami[a,c,d]

Departments of Pathology[a] and Microbiology and Immunology,[b] The Sealy Center for Vaccine Development,[c] The Center for Biodefense and Emerging Infectious Diseases,[d] and Galveston National Laboratory,[e] Galveston, Texas, USA, and The University of Texas Medical Branch, Galveston, Texas, USA, and Special Pathogens Laboratory, Department of Virology 1, National Institute of Infectious Diseases, Gakuen, Musashimurayama, Tokyo, Japan[f]

Rift Valley fever virus (RVFV), belonging to the genus *Phlebovirus*, family *Bunyaviridae*, is endemic to sub-Saharan Africa and causes a high rate of abortion in ruminants and hemorrhagic fever, encephalitis, or blindness in humans. MP-12 is the only RVFV strain excluded from the select-agent rule and handled at a biosafety level 2 (BSL2) laboratory. MP-12 encodes a functional major virulence factor, the NSs protein, which contributes to its residual virulence in pregnant ewes. We found that 100% of mice subcutaneously vaccinated with recombinant MP-12 (rMP12)-murine PKRN167 (mPKRN167), which encodes a dominant-negative form of mouse double-stranded RNA (dsRNA)-dependent protein kinase (PKR) in place of NSs, were protected from wild-type (wt) RVFV challenge, while 72% of mice vaccinated with MP-12 were protected after challenge. rMP12-mPKRN167 induced alpha interferon (IFN-α) in sera, accumulated RVFV antigens in dendritic cells at the local draining lymph nodes, and developed high levels of neutralizing antibodies, while parental MP-12 induced neither IFN-α nor viral-antigen accumulation at the draining lymph node yet induced a high level of neutralizing antibodies. The present study suggests that the expression of a dominant-negative PKR increases the immunogenicity and efficacy of live-attenuated RVFV vaccine, which will lead to rational design of safe and highly immunogenic RVFV vaccines for livestock and humans.

Rift Valley fever (RVF) is a mosquito-borne zoonotic disease caused by Rift Valley fever virus (RVFV) that belongs to the genus *Phlebovirus*, family *Bunyaviridae* (68). RVF has been endemic in sub-Saharan African countries for more than 80 years and has spread to Egypt, Madagascar, Saudi Arabia, and Yemen (6, 7, 12, 68, 71). RVFV causes a high rate of abortion and acute lethal infection in newborn ruminants, such as sheep, goats, and cattle, and febrile illness in humans (13, 68, 71). Although most human patients recover from the disease without any complications, some develop lethal hemorrhagic fever or encephalitis, whereas approximately 1 to 10% of patients experience blindness for undefined periods (25, 61). RVFV is transmitted by mosquitoes; floodwater *Aedes* species maintain RVFV in areas of endemicity through transovarial transmission, whereas other mosquito species belonging to the genus *Culex* or *Anopheles* that bite both ruminants and humans can also transmit RVFV during outbreaks and work as amplification vectors (41, 59). The spread of RVFV into countries where it is not endemic may occur through the spread of RVFV-infected mosquitoes, movement of animals, or travel of humans infected with RVFV or intentional attacks with biological agents (9, 72, 73). RVFV is a risk group 3 pathogen and an overlap select agent of the Department of Health and Human Services (HHS) and the U.S. Department of Agriculture (USDA) and a category A high-priority pathogen of the National Institute for Allergy and Infectious Diseases (NIAID) in the United States (44, 45).

The genome of RVFV is comprised of a tripartite negative-strand RNA genome with S, M, and L segments (68). The S segment encodes the nucleocapsid (N) protein and nonstructural NSs protein in an ambisense manner. The M segment encodes a single M mRNA, and the precursor protein can be cotranslationally cleaved into the 78-kDa protein, the nonstructural protein NSm, and viral envelope proteins Gn and Gc. The L segment encodes the RNA-dependent RNA polymerase. Neither NSs nor NSm is essential for viral replication, and recombinant RVFV lacking both NSs and NSm is still viable (4). The lack of NSm does not affect viral replication in type I interferon (IFN)-competent cells, and the virus still retains its virulence in the rat model (5). On the other hand, lack of NSs abrogates RVFV competency to replicate in type I IFN-competent cells (29, 56), which results in the attenuation of RVFV in animals (10, 14, 74), suggesting that NSs is a major virulence factor of RVFV.

Vaccination of susceptible ruminants and humans is the only effective way to prevent the spread of RVFV during an outbreak (26). Currently, there are no licensed vaccines or therapeutics available outside countries where the virus is endemic. Randall et al. developed a formalin-inactivated vaccine for Rift Valley fever (64). The original inactivated candidate vaccine has been improved in terms of safety by using FRhL-2 cells instead of primary rhesus or African green monkey kidney cells. The improved vaccine, TSI-GSD-200, was produced with the virulent Entebbe strain, and the manufacturing capability at a high-containment

Received 29 March 2012 **Accepted** 30 April 2012
Published ahead of print 9 May 2012
Address correspondence to Tetsuro Ikegami, teikegam@utmb.edu.
O.L. and B.K. contributed equally to this work.
Supplemental material for this article may be found at http://jvi.asm.org/.

doi:10.1128/JVI.00778-12

facility is very limited. Pittman et al. demonstrated that vaccination with TSI-GSD 200 on days 0, 7, and 28 (subcutaneously [s.c.]) elicits a geometric neutralizing antibody titer of 1:237, while the half-life of the neutralizing antibody is 287 days and the titer decreased below 1:40 (62). Because of the requirement for repeated immunization to gain sufficient neutralizing antibody titer and the short half-life of the resulting neutralizing antibodies, it would be ideal to prepare a vaccine candidate that will induce rapid and long-term protective immunity in both humans and ruminants with a single administration, i.e., a live-attenuated vaccine. However, there is concern that live-attenuated vaccine strains may revert to virulence and cause unexpected diseases among vaccinees. Candidate live-attenuated vaccines, the MP-12 strain (11) and the clone 13 strain (C13) (56), have been shown to be immunogenic in ruminants and sufficiently safe for veterinary use (14, 48, 50–55), while the safety evaluations of these vaccines in humans has not been completed. At present, MP-12 is the only RVFV strain that is a risk factor 2 pathogen and that is excluded from the select-agent rule. The MP-12 strain carries attenuated M and L segments, while the S segment encodes a virulent phenotype due to the functional NSs gene (2, 67, 75). The C13 strain carries wild-type RVFV M and L segments, while the S segment encodes NSs with a 69% truncation, which abolishes all functions of NSs (3, 21, 37, 38, 56). Using a reverse genetics system for the MP-12 strain, a recombinant MP-12 (rMP12) with a 69% truncation of the NSs gene that is identical to that of strain C13 NSs was generated and designated rMP12-C13type (29). rMP12-C13type carries attenuated M and L segments of MP-12, while the immunogenicity and efficacy of rMP12-C13type in animals and humans have not been characterized.

RVFV inhibits host general transcription, including beta interferon (IFN-β) mRNA synthesis (3, 37, 38). Transcription factor IIH (TFIIH) is an essential transcription factor for host RNA polymerases I and II (24, 43) and is composed of 10 subunit proteins: XPD (gene defective in xeroderma pigmentosum patient complementation group D), p8, p34, p44, p52, p62, XPB, ménage-à-trois 1 (MAT1), cyclin H, and cdk7 (18, 69). NSs suppresses the general host transcription by sequestering TFIIH p44 subunit proteins (37) and by promoting the degradation of TFIIH p62 subunit proteins (32). In addition to suppressing broad-host-range transcription through interference with TFIIH function, NSs can also bind to Sin3A-associated protein 30 (SAP30) on the IFN-β promoter, which may repress the activation of the promoter (38).

In addition to general transcription suppression, NSs also promotes the degradation of double-stranded RNA (dsRNA)-dependent protein kinase (PKR) (21, 27). During the replication of RNA viruses, PKR binds to dsRNA or 5′-triphosphated single-stranded RNA (ssRNA) at its dsRNA-binding domain, located at the N terminus, which causes a conformational change exposing the kinase domain at the C terminus (17). Active PKR is a dimer and phosphorylates the eIF2α subunit protein (17). eIF2-GTP transports methionine-tRNA to the 43S preinitiation complex to initiate translation, while eIF2B is responsible for converting eIF2-GDP into eIF2-GTP (16). The phosphorylated eIF2α binds to eIF2B at high affinity and sequesters the limited eIF2B molecule (16). Cells with phosphorylated eIF2α cannot initiate translation; however, RVFV NSs degrades PKR and prevents the phosphorylation of eIF2α during viral replication (27). Since suppression of PKR leads to the active synthesis of viral proteins during infection, we hypothesized that MP-12, encoding a dominant-negative form of PKR, would inhibit PKR-mediated eIF2α phosphorylation without suppressing host innate immune responses and effectively induce protective immunity against RVFV. We generated rMP12-murine PKRN167 (mPKRN167), which encodes a dominant-negative form of mouse PKR in place of NSs, and tested its efficacy and immunogenicity in mice.

MATERIALS AND METHODS

Media, cells, and viruses. BHK/T7-9 cells that express T7 RNA polymerase (30) were grown in minimal essential medium alpha (MEM-alpha) containing 10% fetal calf serum (FCS). Penicillin (100 U/ml) and streptomycin (100 μg/ml) were added to the medium. BHK/T7-9 cells were selected in medium containing 600 μg/ml hygromycin. rMP12-C13type, which carries the NSs gene with a 69% in-frame truncation (29), was described previously. rMP12-mPKRN167 encodes the N terminus of mouse PKR from amino acids (aa) 1 to 167 with an N-terminal Flag tag in place of MP-12 NSs. These recombinant MP-12 viruses were recovered from BHK/T7-9 cells as described previously (29) and passaged once in Vero E6 cells. Viral titers were determined by plaque assay in Vero E6 cells. Lyophilized MP-12 vaccine was reconstituted and passaged once either in MRC-5 cells or in Vero E6 cells. RVFV strain ZH501 stock was generated after one Vero E6 cell passage of an original ZH501 reference collection vial (serial number JM1137) at the University of Texas Medical Branch (UTMB) (49).

Plasmids. The N terminus of mouse PKR (aa 1 to 167) with a Flag tag was amplified by PCR from first-strand cDNA, derived from total RNA of wild-type (wt) mouse embryonic fibroblasts (MEFs) that were infected with rMP12-C13type (7 h postinfection [p.i.]), with HpaFlagmPKR-F (5′-TGT CGT TAA CAT GGA TTA CAA GGA TGA CGA CGA TAA GAT GGC CAG TGA TAC CCC AGG T-3′) and Spe-m167-PKR-R (5′-AGG AAC TAG TTC AAG TTT TCG GCG GGC TCT TTA ACA-3′) (restriction enzyme sites are underlined). Then, the PCR fragments that were cut with HpaI and SpeI were cloned into the NSs open reading frame (ORF) of pProT7-vS(+) that was cut with HpaI and SpeI as described previously (29).

Recovery of recombinant MP-12. The rMP12-mPKRN167 virus was recovered in BHK/T7-9 cells by using a plasmid combination of pProT7-S(+)-mPKRN167, pProT7-M(+), pProT7-L(+), pT7-IRES-vN, and pT7-IRES-vL, as described previously (29).

Western blotting. MEFs were mock infected or infected with MP-12, rMP12-C13type, or rMP12-mPKRN167 at a multiplicity of infection (MOI) of 3, and cells were collected into 2× sample buffer at 12 or 16 h p.i. Western blot analysis was performed as described previously (27). The membranes were incubated with anti-eIF2-alpha antibody (Cell Signaling Technology), anti-phospho-eIF2-alpha (ser51) antibody (Cell Signaling Technology), anti-RVFV mouse polyclonal antibody (a kind gift from R. B. Tesh, UTMB), anti-FLAG M2 monoclonal antibody (Sigma), and anti-actin polyclonal antibody (I-19; Santa Cruz Biotechnology).

Immunization and virus challenge. For testing humoral immune responses, 5-week-old female CD1 outbred mice were inoculated subcutaneously with phosphate-buffered saline (PBS) (mock) ($n = 5$) or 1×10^5 PFU of MP-12 ($n = 10$), rMP12-C13type ($n = 10$), or rMP12-mPKRN167 ($n = 10$). At 1, 2, 3, 30, 90, and 180 days p.i., less than 100 μl of blood was collected from the retro-orbital vein, and serum samples were obtained for IFN-α enzyme-linked immunosorbent assay (ELISA), virus plaque assay, or a plaque reduction-neutralization test ($PRNT_{80}$). For testing the efficacy of MP-12 NSs mutants, 5-week-old female CD1 outbred mice were inoculated subcutaneously with PBS (mock) ($n = 10$) or 1×10^5 PFU of MP-12 ($n = 11$), rMP12-C13type ($n = 10$), or rMP12-mPKRN167 ($n = 9$). Sera were collected at 42 days p.i., and the mice were challenged with 1×10^3 PFU of wt RVFV strain ZH501 (intraperitoneally [i.p.]) at 44 days p.i. The challenge experiment was performed at an animal biosafety level 4 (BSL4) facility at the UTMB Shope laboratory. The mice were observed for 21 days, and body weight was monitored daily. Survival curves of mice (Kaplan-Meyer method) were analyzed with the

Graphpad Prism 5.03 program (Graphpad Software Inc.). For testing viral antigen accumulation at draining lymph nodes, 5-week-old female CD1 outbred mice were inoculated in the footpad (30 μl) with PBS (mock) ($n = 3$) or 1×10^5 PFU of MP-12 ($n = 4$), rMP12-C13type ($n = 4$), rMP12-mPKRN167 ($n = 4$), or heat-inactivated MP-12 ($n = 3$). The draining lymph nodes (popliteal and inguinal) were collected at 1 day p.i. and used for antigen capture ELISA. Mice that were vaccinated with MP-12 ($n = 3$) were also tested at 2 and 3 days p.i. For testing cytokines and chemokines in mouse sera, 5-week-old female CD1 outbred mice were inoculated in the footpad (30 μl) with PBS (mock) ($n = 3$) or 1×10^5 PFU of MP-12 ($n = 4$), rMP12-C13type ($n = 4$), or rMP12-mPKRN167 ($n = 4$). Sera were collected at 2 days p.i. and used for Bio-Plex analysis.

Detection of cytokines and chemokines in mouse sera. Serum IFN-α was measured by using a VeriKine Mouse Interferon Alpha ELISA Kit (catalog number 42120; PBL International) according to the manufacturer's instructions. A standard curve of mouse IFN-α control (12.5 to 400 pg/ml) was plotted, and the absorbance (optical density [OD]) at 450 nm of serum samples (1:10) was fit onto the standard curve using Graphpad Prism software.

Detection of cytokines and chemokines in mouse sera. Cytokines and chemokines in mouse sera that were collected at 2 days p.i. were measured by Bio-Plex Pro Mouse Cytokine 23-Plex Assay (Bio-Rad) according to the manufacturer's instructions. Cytokine reference standards (2 to 32,000 pg/ml) that were provided by the manufacturer were included in the assay. Mouse sera (15 μl) and universal sample diluents in the kit (45 μl) were mixed and loaded onto a 96-well plate containing beads (each 50 μl). The raw data were first statistically compared by two-way analysis of variance (ANOVA), and the fold difference from mock-infected samples was analyzed subsequently.

Construction of recombinant baculovirus carrying the RVFV N protein gene. A PCR fragment carrying the MP-12 N ORF was cloned into the baculovirus transfer vector pBACgus-1 (Novagen) under the control of the very late strong polyhedrin promoter. This vector carries the GUS reporter gene, which allows selection of recombinant viruses. The RVFV N gene was cloned in frame with a C-terminal His tag fusion sequence presented in the transfer vector. In order to increase the affinity of the recombinant protein for Ni-nitrilotriacetic acid (NTA) resin during the purification process, an additional 6-His sequence was added, separating the vector-derived His tag with a 15-amino-acid linker (34). The constructed transfer vector was designated pBACgus-RVN. Sf9 cells were cotransfected with BacVector-3000 Triple Cut Virus DNA (Novagen) and the transfer vector pBACgus-RVN by using ExGene 500 transfection reagent as described previously (40, 57). Direct plaque purification was used to select recombinant baculovirus clones. X-GlcA substrate was added to the agarose overlay, and blue plaques were selected. The expression of the RVFV N protein was confirmed by indirect immunofluorescence assay (IFA) with anti-RVFV antibody, and the resulting recombinant baculovirus was designated rAcMNPV-RVN.

Expression and purification of RVFV N protein. HighFive cells were infected at an MOI of 5 and collected at different time points, starting at 3 days p.i. The maximum RVFV N protein expression was determined at 6 days p.i. Fifty milliliters of HighFive cell culture was infected at an MOI of 5, and cells were harvested at 6 days p.i. and lysed on ice for 30 min in lysis buffer (8 M urea, 0.1 M NaH_2PO_4, 0.01 M Tris-HCl, pH 8.0) at a 1:5 ratio of cells to buffer. The lysate was clarified by centrifugation, and Ni-NTA HisBind Superflow Resin (EMD4BioSciences) was added to the supernatant. After overnight incubation, the resin was washed with washing buffer 1 (8 M urea, 0.1 M NaH_2PO_4, 0.01 M Tris-Cl, pH 6.3) twice. Nonspecifically bound protein was further removed from the resin by washing with washing buffer 2 (8 M urea, 0.1 M NaH_2PO_4, 0.01 Tris-Cl, pH 5.9), and RVFV N protein was eluted with elution buffer (8 M urea, 0.1 M NaH_2PO_4, 0.01 M Tris-Cl, pH 4.5). The purified N was diluted with PBS for IgG ELISA.

Expression and purification of RVFV NSs protein. The PCR fragment encoding the partial NSs at the C terminus (aa 219 to 265) was amplified with the primer set GST-NSdel3F (5′-CTC AGG ATC CCC ATG GAG GAG AGC CTG ATG CTG CGC TC-3′) (the BamHI site is underlined) and GST-NSdel3R (5′-GCC TGA ATT CCT AAT CAA CCT CAA CAA ATC CAT CAT CAT C-3′) (the EcoRI site is underlined) and cloned downstream of GST between BamHI and EcoRI in the pGEX-3X plasmid (GE Healthcare). Purification of the partial NSs GST fusion protein was performed as described previously (28).

IgG ELISA. RVFV N or NSs protein was expressed and purified as described above, and 96-well ELISA plates were coated overnight at 4°C at a concentration of 100 ng/well. After washing 3 times with PBS containing 0.1% Tween 20 (PBS-T), the wells were blocked with PBS-T containing 5% skim milk at 37°C for 2 h. Then, the wells were incubated with serum samples at 37°C for 1 h. The wells were washed 3 times with PBS-T and reacted with horseradish peroxidase (HRP)-conjugated anti-mouse IgG (Santa Cruz Technologies) at 37°C for 1 h. After washing with PBS-T 3 times, 2,2′-azinobis[3-ethylbenziazoline-6-sulfonic acid] (ABTS) was added to the wells. The plate was incubated at room temperature for 30 min, and the optical density at 415 nm was recorded. The cutoff value, 0.36, was defined as the mean plus 2 times the standard deviation of 36 normal mouse serum samples (1:400) for anti-N IgG, while the cutoff value of 0.144 was defined as the mean plus 3 times the standard deviation of 24 normal mouse serum samples (1:100) for anti-NSs IgG. The highest dilution of sera that gave an OD value larger than the cutoff was designated the anti-N antibody titer. Because the anti-NSs antibody level was low, an OD value of 1:100 dilution was used for demonstrating the presence of anti-NSs antibody.

Antigen-capture ELISA. Mock-infected or RVFV-infected MEFs (2.5×10^5 cells) were incubated with PBS containing 1% Triton X-100 and 0.05% Tween 20 for 10 min at room temperature and centrifuged at 15,000 × *g* at 4°C for 5 min. The supernatants were mixed 1:1 with PBS containing 0.05% Tween 20 and 1% skim milk, and 4-fold serial dilutions were performed. Mouse popliteal and inguinal lymph nodes were collected separately into tubes containing 120 μl of PBS with 1% Triton X-100, 0.05% Tween 20, and 1% skim milk on ice. After homogenization, samples were centrifuged at 15,000 × *g* at 4°C for 5 min. Then, 100 μl of lysate sample was used for ELISA. Antigen capture ELISA was performed as described previously (15), and a 96-well flat-bottom plate was coated with 125 ng of monoclonal antibody (D5-59) against RVFV N in PBS overnight at 4°C. After washing 3 times with PBS-T, the wells were blocked with PBS-T containing 5% skim milk for 2 h at room temperature. Subsequently, lymph node lysates were added to the well and incubated at 37°C for 1 h. The plate was washed with PBS-T 3 times, and rabbit anti-RVFV serum (1:1,000) was added as a detection antibody and incubated at 37°C for 1 h. After washing with PBS-T 3 times, the wells were reacted with HRP-labeled anti-rabbit IgG at 37°C for 1 h. After washing with PBS-T 3 times, ABTS substrate (ABTS tablet and buffer; Roche Diagnostics) was added to the wells. The plate was incubated at room temperature for 30 min, and the optical density at 415 nm was recorded. The cutoff value was determined as the mean plus 3× the standard deviation of 24 wells (MEF cell samples) or 40 wells (lymph node samples) per plate that reacted to PBS instead of the samples.

Plaque reduction neutralization test. Mouse sera (6 μl) and Dulbecco's modified Eagle's medium (DMEM) containing 10% fetal bovine serum (FBS) (42 μl) were mixed and subsequently serially diluted 4-fold. Each 20-μl aliquot of diluent was transferred into flat-bottom 96-well plates containing 5 μl of MP-12 virus (50 PFU/well; final dilutions of sera, 1:10, 1:40, and 1:160). The plate was incubated at 37°C for 1 h, and 150 μl of DMEM with 10% FBS was added to the well. Then, 150 μl of the mixture was transferred into a 24-well plate with confluent Vero E6 cells, and the plate was incubated at 37°C for 1 h. After removal of the inocula, 0.5 ml of a 1:1 mixture of 1.2% Noble agar in water and 2× MEM (Gibco) was overlaid in each well. At 2 days p.i., 0.5 ml of the second overlay, containing neutral red, was added to each well and incubated overnight. The average of the plaque numbers in 6 different wells with added mock-vaccinated mouse sera was used as the cutoff number (typically 8 to 9).

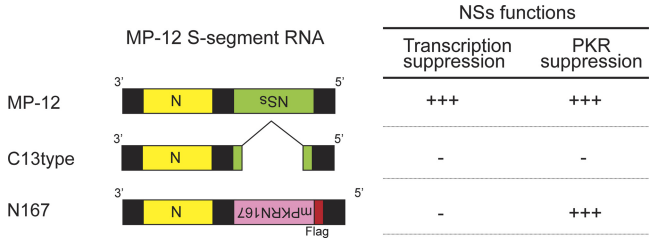

FIG 1 Schematics of S segments of MP-12, rMP12-C13type, and rMP12-mPKRN167. rMP12-C13type (C13type) lacks 69% of the NSs ORF, as described previously (56). rMP12-mPKRN167 (N167) encodes a dominant-negative form of mouse PKR in place of NSs. The expected phenotype corresponding to each S segment is also presented. +++ and − represent the presence and absence of suppression, respectively.

The highest dilution of sera that produced a number of plaques below the cutoff number was designated the $PRNT_{80}$ neutralizing antibody titer.

Detection of RVFV N antigens at popliteal lymph nodes by IFA. Popliteal lymph nodes were collected from mice that were mock vaccinated with PBS or subcutaneously vaccinated with 1×10^5 PFU of MP-12, rMP12-C13type, rMP12-mPKRN167, or heat-inactivated MP-12 (56°C for 30 min) at 1 day p.i. These lymph nodes were fixed overnight with 4% paraformaldehyde, and the fixative was replaced with PBS. The PBS was gradually replaced with 30% sucrose at 4°C and embedded into OCT compound (Sakura Finetek). Cryosectioning was performed at 5-μm thickness, and the sections were fixed with cold acetone-methanol (1:1) for 1 min. Antigens were retrieved with proteinase K (ready to use; Dako catalog number S3020) for 5 min and stained with anti-RVFV N rabbit polyclonal antibody (1:500) (49) or biotin-conjugated anti-CD45R/B220 rat IgG2a antibody (1:500) (clone RA3-6B2; BioLegend) for 2 h at room temperature. Signals were detected by fluorescein isothiocyanate (FITC)-conjugated donkey anti-rabbit IgG (1:1,000; Poly4064; BioLegend) or streptavidin-DyLight 594 (1:1,000; catalog number 405222; BioLegend) by incubating for 30 min at room temperature. Normal rabbit serum (catalog number R9133; Sigma) or biotin rat IgG2a(κ) isotype control (clone RTK2758; BioLegend) was used as the control stain. Specific signals were detected under an Olympus IX71 microscope with a DP71 camera, and the image was detected in DP Manager software.

Statistical analysis. The statistical analyses were performed using the Graphpad Prism 5.03 program (Graphpad Software Inc.). The Mann-Whitney U test and unpaired Student's *t* test were used for the comparison of two groups, while a Kruskal-Wallis test following Dunn's posttest was performed to compare more than three groups. Survival curves of mice were analyzed by a log rank (Mantel-Cox) test.

Ethics statement. Mouse studies were performed in facilities accredited by the Association for Assessment and Accreditation of Laboratory Animal Care (AAALAC) in accordance with the Animal Welfare Act, NIH guidelines, and U.S. federal law. The animal protocol was approved by the UTMB Institutional Animal Care and Use Committee (IACUC) (protocol numbers 0904027 and 1007038). All the recombinant DNA and RVFV were created upon approval of the Notification of Use by the Institutional Biosafety Committee at UTMB. The wt RVFV ZH501 strain was used at the Robert E. Shope BSL4 laboratory at the UTMB in accordance with NIH guidelines and U.S. federal law.

RESULTS

Generation of recombinant MP-12 encoding dominant-negative mouse PKR. Recombinant RVFV strain MP-12 was generated by a reverse genetics system (29). The schematics of MP-12 S segments are shown in Fig. 1. rMP12-C13type carries a 69% in-frame truncation of the NSs gene in the MP-12 backbone (29). rMP12-mPKRN167 encodes the N-terminal 167 amino acids of mouse PKR in place of NSs, which is similar to a dominant-negative form of human PKR, PKRΔE7 (27, 39). To confirm the dominant-negative effect of the mouse PKR N terminus, MEFs were mock infected or infected with MP-12, rMP12-C13type, or rMP12-mPKRN167 at an MOI of 3. Cells were collected at 12 h p.i. or 16 h p.i., and the increase of eIF2α phosphorylation was analyzed. At 12 h p.i., Flag-tagged mouse PKR N terminus was expressed, and the phosphorylation level of eIF2α was similar to that of mock- or MP-12-infected cells, while eIF2α was significantly phosphorylated in cells infected with rMP12-C13type, which lacks a functional NSs gene (Fig. 2A). At 16 h p.i., no increase of eIF2α phosphorylation was observed in cells infected with rMP12-mPKRN167 (Fig. 2B). The results suggest that rMP12-mPKRN167 expresses a dominant-negative form of mouse PKR and inhibits PKR-mediated eIF2α phosphorylation, which is induced in MP-12-infected cells in the absence of NSs.

We noted an apparent increase in N abundance in cells infected with rMP12-mPKRN167 (Fig. 2A). To confirm this, we performed antigen capture ELISA to detect N proteins (15). MEFs were mock infected or infected with MP-12, rMP12-C13type, or rMP12-mPKRN167 at an MOI of 3. Cell lysates were collected at 1 h p.i. and 16 h p.i., and the N abundances were tested by ELISA. At 1 h p.i., similar amounts of N protein were observed among cells infected with MP-12, rMP12-C13type, or rMP12-mPKRN167 (Fig. 2C). At 16 h p.i., more N proteins were accumulated in cells infected with rMP12-mPKRN167 than in those infected with MP-12 or rMP12-C13type (Fig. 2D). The N proteins were not increased in the absence of viral replication (Fig. 2E). These results suggest that the expression of a dominant-negative form of mouse PKR increases the accumulation of N proteins in infected cells. Next, we compared the immunogenicity and efficacy of rMP12-mPKRN167 with those of parental MP-12 or rMP12-C13type.

Efficacy and immunogenicity of rMP12-mPKRN167. To know whether the expression of dominant-negative PKR supports the immunogenicity of MP-12 vaccine, we first analyzed the levels of IFN-α, viremia, and neutralizing antibodies in vaccinated mice. Mice were subcutaneously vaccinated with PBS or 1×10^5 PFU of MP-12, rMP12-C13type, or rMP12-mPKRN167. Viruses were inoculated in the common dorsal subcutaneous area so that the efficacy data would be comparable to those of other vaccine candidates using subcutaneous inoculation. All the mice vaccinated with rMP12-mPKRN167 induced detectable IFN-α in the sera at 1 day p.i., whereas 0 or 55% of mice vaccinated with MP-12 or rMP12-C13type, respectively, induced IFN-α (Fig. 3A). Viremia levels in sera at 1, 2, and 3 days p.i. were tested by plaque assay. Three of 10 mice that were vaccinated with MP-12 developed viremia of 100 to 400 PFU/ml at 3 days p.i., while no mice that were vaccinated with rMP12-C13type or rMP12-mPKRN167 virus showed detectable viremia of 100 PFU/ml or more (Fig. 3B). These results suggest that a lack of NSs in MP-12 resulted in the induction of type-I IFN in mice and prevented viremia.

We tested the development of neutralizing antibody in vaccinated mice at day 30, day 90, and day 180 to determine the effect of dominant-negative PKR expression on long-term immunity (Fig. 3C). The mean neutralizing antibody titers of mice that were vaccinated with MP-12, rMP12-C13type, or rMP12-mPKRN167 were highest at 90 days p.i. and were 1:2,988, 1:1,056, or 1:2,497, respectively, while the mean neutralizing antibody titers were decreased to 1:1,068, 1:216, or 1:961, respectively, at 180 days p.i. All mice vaccinated with rMP12-mPKRN167 induced neutralizing antibody at 90 days p.i., while 3 or 1 mouse vaccinated with MP-12

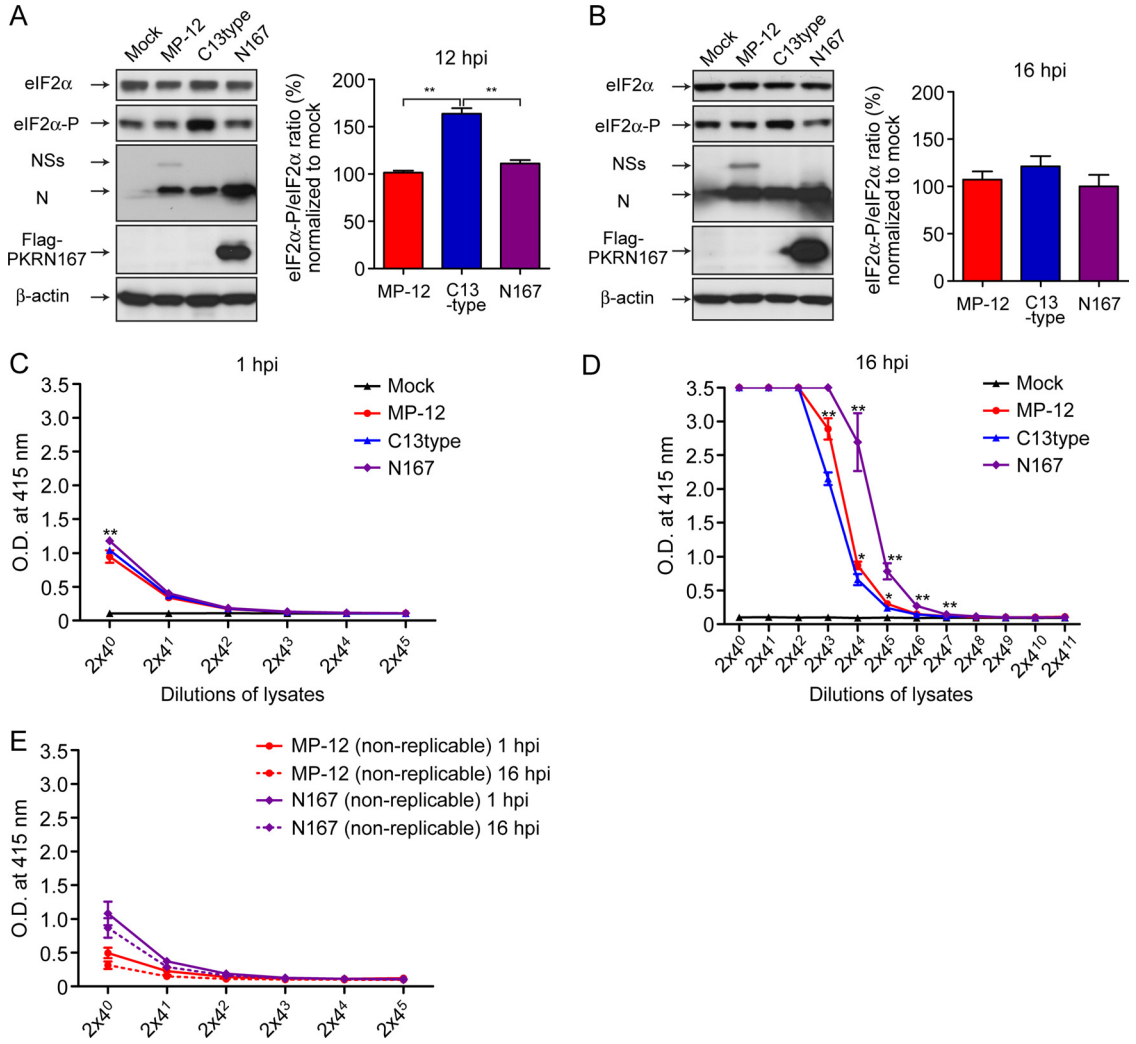

FIG 2 Dominant-negative effect of rMP12-mPKRN167. Wild-type MEFs were mock infected or infected with MP-12, rMP12-C13type, or rMP12-mPKRN167 at an MOI of 3. Cells were collected at 12 h p.i. (A) or 16 h p.i. (B), and the abundance of eIF2α, phosphorylated eIF2α (eIF2α-P) (Ser 51), NSs, N, Flag-PKR N167, and β-actin were analyzed by Western blotting. The mean ratios and standard deviations of the density of phosphorylated eIF2α and eIF2α were determined from 3 independent experiments. The asterisks represent statistical significance (Student's unpaired *t* test; $P < 0.01$). (C and D) MEFs were mock infected or infected with MP-12, rMP12-C13type, or rMP12-mPKRN167 at an MOI of 3. Cell lysates were collected at 1 h p.i. (C) and 16 h p.i. (D), and the abundance of N proteins was measured by antigen capture ELISA for RVFV N proteins (15). The asterisks represent statistical significance (Mann-Whitney U test; *, $P < 0.05$; **, $P < 0.01$ versus rMP12-C13type at each dilution). (E) As a control to monitor initial N protein derived from inocula, heat-inactivated MP-12 or rMP12-mPKRN167 was also tested.

or rMP12-C13type, respectively, did not induce neutralizing antibodies. These results suggest that the expression of dominant-negative PKR is an effective way to successfully induce long-term neutralizing antibodies by using MP-12 vaccines lacking NSs.

We next tested the efficacy of rMP12-mPKRN167 in mice. Outbred CD1 mice were mock vaccinated with PBS or vaccinated with 1×10^5 PFU of MP-12, rMP12-C13type, or rMP12-mPKRN167 via the subcutaneous route. At 44 days p.i., mice were challenged with 1×10^3 PFU of wt RVFV ZH501 (i.p.), and survival was monitored for 21 days. Mock-vaccinated mice succumbed to RVFV-induced disease within 10 days p.i. (mean survival time, 8 days), while all mice vaccinated with rMP12-mPKRN167 were protected from wt RVFV challenge (Fig. 4A). On the other hand, 72% or 80% of mice vaccinated with MP-12 or rMP12-C13type, respectively, were protected from challenge (Fig. 4A). We did not find statistical significance by the log rank test in the survival curve among the vaccinated mice. The daily weight change showed a continuous decrease in body weight in mock-vaccinated mice, while surviving mice that were vaccinated with MP-12, rMP12-C13type, or rMP12-mPKRN167 did not show a significant decrease in body weight after wt RVFV challenge (Fig. 4B). Further, we determined neutralizing antibody titers prior to challenge with wt RVFV at 42 days postimmunization. Importantly, all of the vaccinated mice that succumbed to disease lacked detectable neutralizing antibodies at 42 days p.i. (Table 1). These results suggest that neutralizing antibody plays an important role in protecting vaccinated animals from wt RVFV challenge. We also noticed that one mouse that was vaccinated with rMP12-mPKRN167 (number 10-1) survived without detectable neutralizing antibodies at 42 days p.i. (Table 1). The sera were

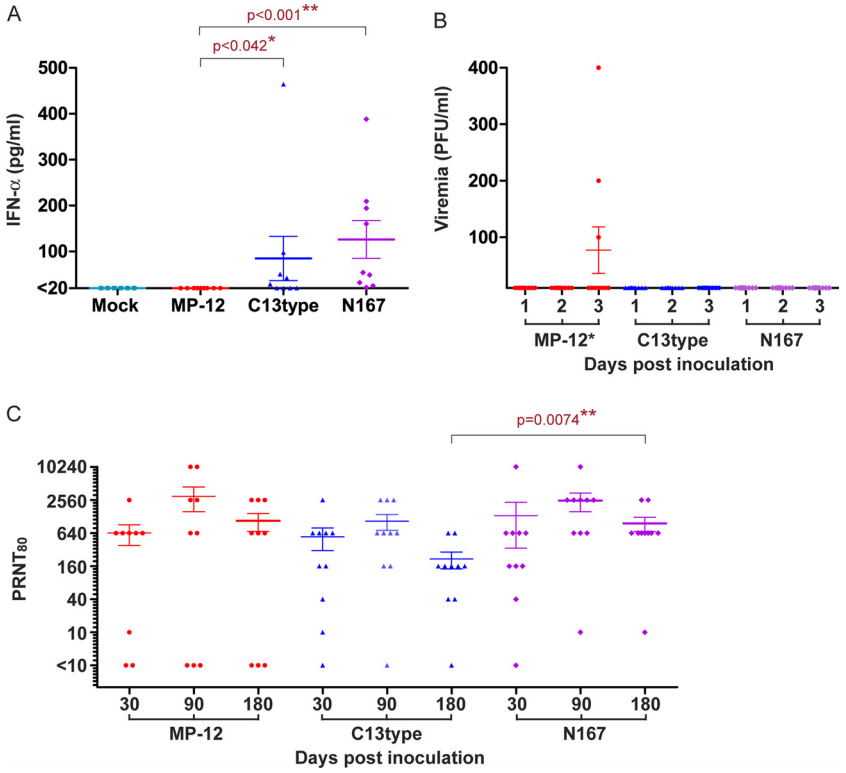

FIG 3 Immunogenicity of rMP12-mPKRN167. Five-week-old CD1 mice were mock vaccinated with PBS ($n = 6$) or vaccinated subcutaneously with 1×10^5 PFU of MP-12, rMP12-C13type (C13type), or rMP12-mPKRN167 (N167) ($n = 9$). Sera were collected at 1, 2, 3, 30, 90, and 180 days p.i. (A) Abundance of IFN-α in mouse serum samples (mock, $n = 6$; other groups, $n = 9$) at 1 day p.i. Serum IFN-α was measured with the VeriKine Mouse Interferon Alpha ELISA Kit (PBL International). A Mann-Whitney U test was performed for statistical analyses (*, $P < 0.05$; **, $P < 0.01$). (B) Viral titers of mouse serum samples ($n = 10$ per group). The viral titers in serum samples at days 1, 2, and 3 were determined by plaque assay in Vero E6 cells. *, $P < 0.05$ by the Kruskal-Wallis test. (C) Neutralizing antibody titers of serum samples: MP-12 ($n = 9$), C13type ($n = 10$), or N167 ($n = 10$). A $PRNT_{80}$ was performed to determine the neutralizing antibody titer. A Mann-Whitney U test was performed for statistical analyses between $PRNT_{80}$ titers at 180 days p.i. (*, $P < 0.05$; **, $P < 0.01$). The error bars indicate standard deviations.

further analyzed with an IgG ELISA system to detect anti-N-specific antibodies. We found that the survivor (number 10-1) lacking neutralizing antibody had a 1:1,600 titer of anti-N antibodies (Table 1). It was also found that three dead mice that were vaccinated with MP-12 (number 3-1, 3-4, and 4-4) lacked both detectable neutralizing antibodies and anti-N IgG (Table 1), indicating that MP-12 failed to stimulate the host immune system in those mice.

In addition to immunogenicity, the ability to differentiate infected from vaccinated animals (DIVA) is important for vaccine development. MP-12 lacks a marker for DIVA, and antibody responses cannot be discriminated from natural infection. rMP12-

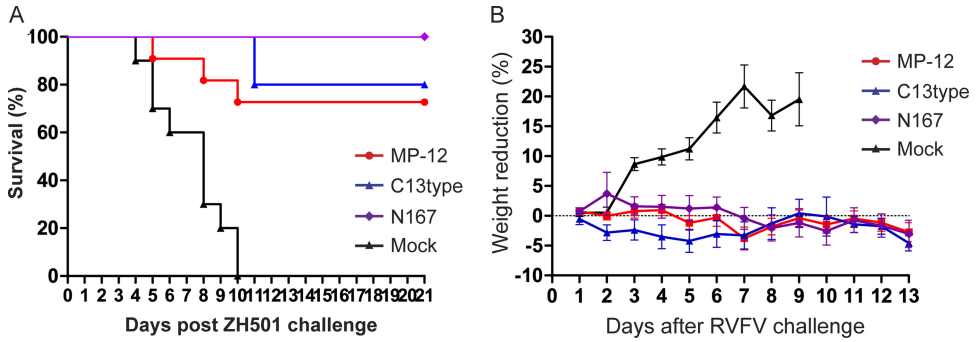

FIG 4 Protection efficacy of rMP12-mPKRN167 in mice. Five-week-old CD1 mice were mock vaccinated ($n = 10$) or vaccinated subcutaneously with 1×10^5 PFU of MP-12 ($n = 10$), rMP12-C13type (C13type) ($n = 10$), or rMP12-mPKRN167 (N167) ($n = 9$). Sera were collected at 42 days p.i., and mice were challenged with 1×10^3 PFU of wt RVFV strain ZH501 (i.p.) at 44 days p.i. The mice were observed for 21 days postchallenge. (A) Kaplan-Meier survival curves of vaccinated mice after wt RVFV challenge. (B) Daily weight changes of mock-vaccinated mice or surviving vaccinated mice after challenge. The error bars indicate standard deviations.

TABLE 1 Antibody titers pre- and post-wt RVFV challenge

Virus	Mouse no.	Pre-challenge[a]			Death day	Postchallenge[b] anti-NSs OD value[c]
		$PRNT_{80}$ titer	Anti-N titer	Anti-NSs OD value[c]		
MP-12	3-1	<10	<1:100	0.123	8	
	3-2	10,240	1:102,400	0.238		0.190
	3-3	640	1:102,400	0.175		0.207
	3-4	<10	<1:100	0.098	10	
	3-5	2,560	1:51,200	0.105		0.134
	4-1	2,560	1:102,400	0.436		0.353
	4-2	10,240	1:25,600	0.105		0.155
	4-3	2,560	1:51,200	0.098		0.143
	4-4	<10	<1:100	0.106	5	
	4-5	2,560	>1:204,800	0.111		0.173
	11-1	10,240	1:3,200	0.106		0.178
C13type	5-1	2,560	1:102,400	0.105		0.297
	5-2	<10	1:3,200	0.127	10	
	5-3	160	1:12,800	0.103		0.159
	5-4	40	1:12,800	0.104		0.247
	5-5	<10	1:12,800	0.110	10	
	6-1	640	1:12,800	0.120		0.356
	6-2	40	1:12,800	0.108		0.217
	6-3	40	1:400	0.120		0.118
	6-4	640	1:12,800	0.106		0.187
	6-5	10	1:3,200	0.114		0.134
N167	9-1	2,560	>1:204,800	0.104		0.228
	9-2	40	1:6,400	0.105		0.179
	9-3	40	1:3,200	0.106		0.188
	9-4	160	1:3,200	0.098		0.158
	9-5	10,240	1:102,400	0.108		0.179
	10-1	<10	1:1,600	0.104		0.344
	10-2	40	1:6,400	0.102		0.125
	10-3	160	1:3,200	0.098		0.117
	10-4	2,560	1:6400	0.101		0.204

[a] Prechallenge, 42 days postimmunization.
[b] Postchallenge, 21 days postchallenge.
[c] OD value of sera diluted at 1:100. The cutoff value was determined to be 0.144 in this experiment.

C13type and rMP12-mPKRN167 encode a negative DIVA marker (lack of the NSs gene). We tested whether vaccinated mice induce anti-NSs antibody. For this purpose, we developed an IgG ELISA by using truncated NSs proteins that were tagged with GST at the N terminus to detect IgG that was specific to NSs. NSs is a nonstructural protein and is expressed only when virus replicates in cells. Although MP-12 encodes NSs, only 3 out of 11 mice vaccinated with MP-12 raised anti-NSs IgG (Table 1), while none of the mice vaccinated with rMP12-C13type or rMP12-mPKRN167 developed detectable anti-NSs antibodies before challenge. These results suggest that rMP12-C13type and rMP12-mPKRN167 are superior to MP-12 in DIVA. After wt RVFV challenge, 6 out of 8 (75%) or 7 out of 9 (77.7%) mice vaccinated with rMP12-C13type or rMP12-mPKRN167 raised detectable anti-NSs antibodies (Table 1). The OD value of anti-NSs antibodies in pre- and postchallenge sera were statistically significant (Mann-Whitney U test; $P < 0.01$) in mice vaccinated with rMP12-C13type and rMP12-mPKRN167, but not in those vaccinated with MP-12.

Impact of dominant-negative PKR on viral-protein accumulation. PKR suppression promotes viral-protein accumulation and replication of RVFV in cell culture (27). To understand why rMP12-mPKRN167 has high efficacy in mice, we tested the accumulation of viral proteins at the local draining lymph nodes. We chose to observe popliteal and inguinal lymph nodes after vaccination in the footpad, because the antigen accumulation at those draining lymph nodes is well characterized in mice (22). Outbred CD1 mice were mock vaccinated or vaccinated with 1×10^5 PFU of MP-12, rMP12-C13type, or rMP12-mPKRN167 subcutaneously in the footpads. Then, popliteal and inguinal lymph nodes were separately collected to measure the abundance of RVFV N antigens. Before the assay, we analyzed the amounts of RVFV N antigens in virus inocula by using antigen capture ELISA, which can specifically detect RVFV N (15). Figure 5A shows the OD values of virus inocula containing MP-12, rMP12-C13type, rMP12-mPKRN167, or heat-inactivated MP-12 (a control virus that cannot replicate). We confirmed that N abundances were similar among the inocula. The cutoff value of the ELISA was determined for each plate as the mean plus 3 times the standard deviation of 40 wells that reacted to PBS instead of samples. At 1 day p.i., the popliteal lymph nodes of mice vaccinated with C13type (4 out of 4; 100%) or N167 (4 out of 4; 100%) showed significant N protein accumulation (Fig. 5B), whereas the N proteins were only marginally increased in popliteal lymph nodes of mice that were vaccinated with MP-12 (3 out of 4; 75%) (Fig. 5B).

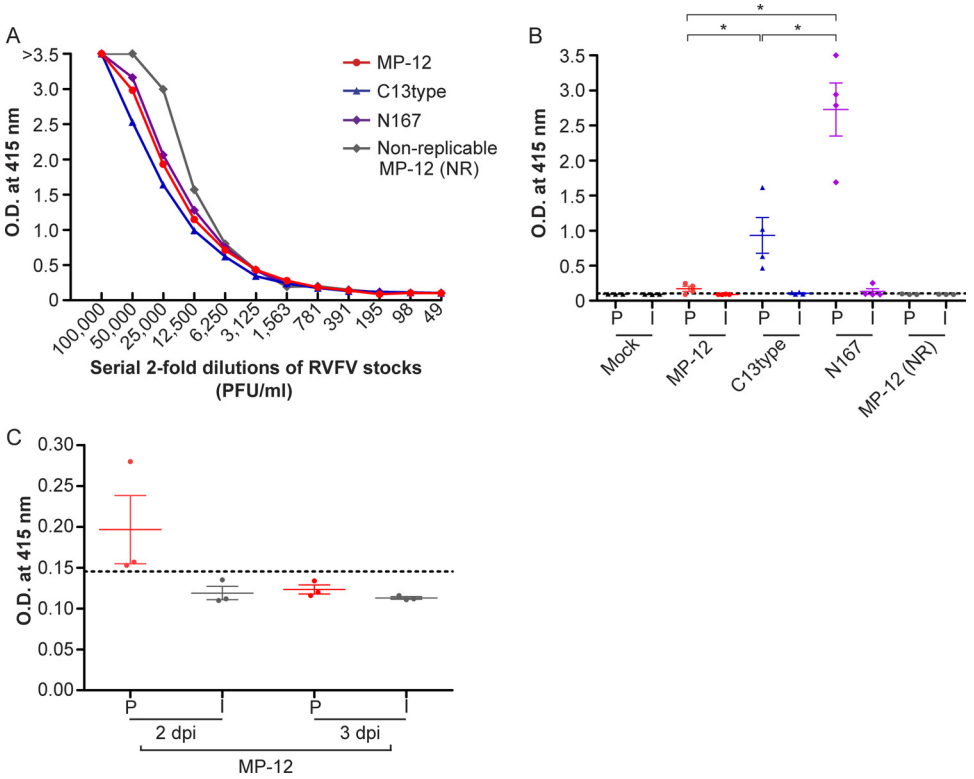

FIG 5 Viral N protein accumulation in the draining lymph nodes of mice after immunization. (A) Relative abundance of RVFV N in viral stocks prepared from Vero E6 cells. Representative data from three independent experiments are shown. (B) Five-week-old outbred CD1 mice were mock vaccinated with PBS or vaccinated in the footpad with 1×10^5 PFU (30 μl) of MP-12, rMP12-C13type (C13type), or rMP12-mPKRN167 (N167) or heat-inactivated nonreplicable (NR) MP-12 at 56°C for 30 min. Popliteal (P) and inguinal (I) lymph nodes were collected at 1 day p.i., and the lysates were used for antigen capture ELISA. The cutoff of 0.104 is shown as a dotted line. The asterisk represents statistical significance (Mann-Whitney U-test; $P < 0.05$). (C) Antigen capture ELISA was performed by using popliteal and inguinal lymph nodes of mice vaccinated with MP-12, which were collected at 2 and 3 days p.i. The cutoff value of 0.145 is shown as a dashed line. The error bars indicate standard deviations.

The N protein was significantly increased in mice vaccinated with rMP12-mPKRN167 compared to rMP12-C13type, suggesting that dominant-negative PKR expression promotes the synthesis of viral proteins. On the other hand, only a marginal increase of N proteins was observed in inguinal lymph nodes derived from mice vaccinated with rMP12-C13type or rMP12-mPKRN167. Since no increase of N protein was observed in popliteal lymph nodes of mice that were vaccinated with heat-inactivated nonreplicable MP-12, N protein most likely accumulates as a result of virus replication. We also tested the accumulation of RVFV N protein in the draining lymph nodes of mice that were vaccinated with MP-12 at day 2 or 3 postimmunization. N proteins from the popliteal lymph nodes of mice vaccinated with MP-12 were detected at 2 days p.i., while they were no longer detected at 3 days p.i. (Fig. 5C), suggesting that RVFV N protein accumulates poorly in draining lymph nodes of mice vaccinated with MP-12.

Because we did not know how RVFV antigens accumulated in popliteal lymph nodes of mice that were infected with rMP12-C13type or rMP12-mPKRN167 virus, we analyzed antigen localization in frozen sections of popliteal lymph nodes derived from mock-vaccinated mice or mice vaccinated with MP-12, rMP12-C13type, rMP12-mPKRN167, or heat-inactivated MP-12 ($n = 3$) by IFA with anti-RVFV N antibody (green) and anti-CD45R/B220 antibody (red; B cell marker). No signals were detected by using a mixture of control antibodies (Fig. 6A). RVFV N antigens were not detected in sections derived from mock-vaccinated mice (Fig. 6B) or mice vaccinated with MP-12 or heat-inactivated MP-12, while a few N-positive cells were detected in the popliteal lymph nodes of mice vaccinated with rMP12-C13type (Fig. 6F). Sections from mice that were vaccinated with rMP12-mPKRN167 consistently showed several cells that were positive to anti-RVFV N antibody in the frozen section (Fig. 6C to E). Cells with RVFV N antigens were found in the T cell zone surrounding B cell follicles (Fig. 6E) or the subcapsular sinus (Fig. 6C), as well as inside B cell follicles (Fig. 6D). Cells containing RVFV N antigens were distinct from lymphocytes in shape, and the diameter reached approximately 30 μm with interdigitated cytoplasm, contacted surrounding lymphocytes, and was morphologically similar to that of dendritic cells (DCs). Sections were also stained with anti-RVFV N antibody and anti-CD207/langerin antibody, which is a specific marker of epidermal Langerhans cells (LCs), migratory LCs, or langerin$^+$ DCs (47); however, RVFV N-positive cells did not show significant staining with anti-CD207/langerin antibody over background levels (data not shown). In single-cell suspensions that were derived from popliteal lymph nodes of mice that were infected with rMP12-GFP, which encodes green fluorescent protein (GFP) in place of NSs (29), we confirmed that cells infected with RVFV were stained with anti-CD11c antibody but not with anti-CD207/langerin antibody (see Fig. S1 in the supplemental

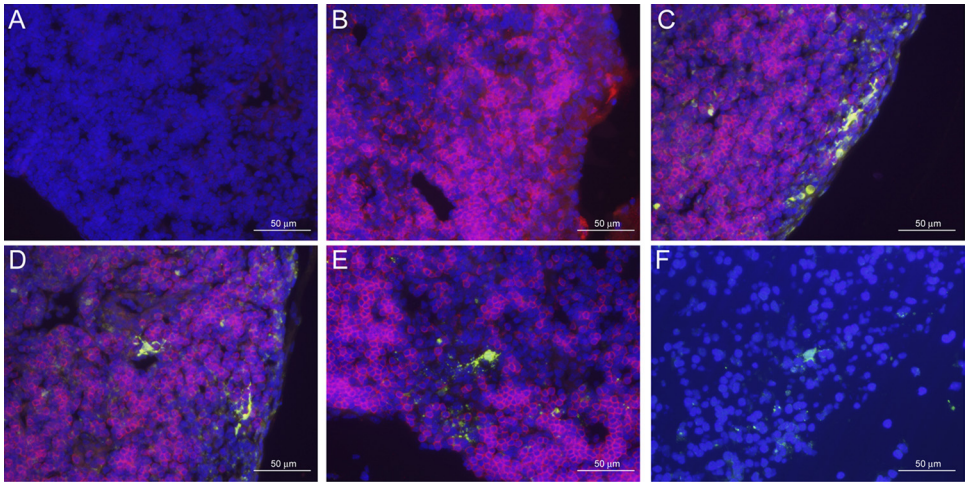

FIG 6 Localization of RVFV N antigens at the draining lymph nodes. Popliteal lymph nodes of mice that were mock vaccinated (B) or vaccinated with rMP12-mPKRN167 virus (A and C to E) or rMP12-C13type (F) were stained with a mixture of control antibodies (normal rabbit serum and biotin-conjugated anti-rat IgG2a) (A), a mixture of anti-RVFV N antibody and biotin-conjugated anti-CD45R/B220 antibody (B to E), or anti-RVFV N antibody only. Nuclei were counterstained with DAPI (4′,6-diamidino-2-phenylindole). The scale is indicated in each panel.

material). These results suggest that DCs infected with rMP12-mPKRN167 are accumulated in draining lymph nodes after immunization.

Cytokine and chemokine induction by MP-12 and mutants. To gain further insight into the ability of MP-12 to stimulate the host immune system, we analyzed the cytokine and chemokine levels in mouse sera at 2 days p.i. Outbred CD1 mice were vaccinated s.c. in the footpad with PBS or 1×10^5 PFU of MP-12, rMP12-C13type, or rMP12-mPKRN167 as for lymph node analyses, and sera were collected 2 days p.i. Serum cytokines were directly detected with the Bio-Plex Pro Mouse Cytokine 23-Plex Assay. Interleukin 5 (IL-5) was increased in mice vaccinated with rMP12-mPKRN167, while other cytokines or chemokines were not significantly increased (Fig. 7). On the other hand, mice vaccinated with MP-12 had increased IL-5; IFN-γ; IL-17; granulocyte macrophage colony-stimulating factor (GM-CSF); macrophage inflammatory protein 1β (MIP-1β); regulated on activation, normal T cell expressed and secreted (RANTES); keratinocyte chemoattractant (KC); and eotaxin compared to a mock-infected control (Fig. 7). These results suggest that MP-12 induces cytokines and chemokines in sera, although MP-12 accumulates poorly at draining lymph nodes. Collectively, it suggests that MP-12 stimulates host immune responses in a manner distinct from that of rMP12-C13type or rMP12-mPKRN167, which lack NSs.

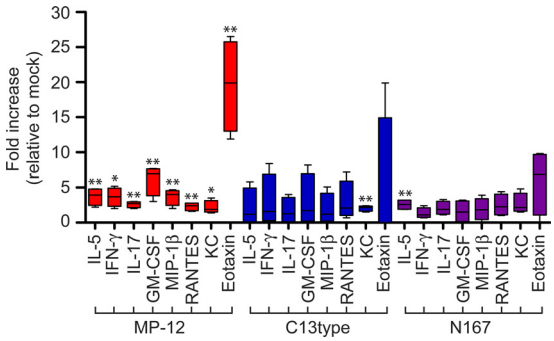

FIG 7 Measurement of cytokines and chemokines in the sera of vaccinated mice. Five-week-old CD1 mice were mock vaccinated with PBS ($n = 3$) or vaccinated in the footpad with 1×10^5 PFU (30 μl) of MP-12, rMP12-C13type (C13type), or rMP12-mPKRN167 (N167) ($n = 4$). Sera were collected at 2 days p.i., and the abundance of cytokines and chemokines was measured by using the Bio-Plex Pro Mouse Cytokine 23-Plex Assay (Bio-Rad). The fold increases relative to the highest values of mock samples are shown. An unpaired Student's *t* test (versus mock vaccinated) was performed for statistical comparison (*, $P < 0.05$; **, $P < 0.01$). The error bars indicate standard deviations.

DISCUSSION

The RVFV MP-12 strain is one of the most immunogenic candidate live-attenuated vaccines for Rift Valley fever in animals and the only RVFV strain that is excluded from the select-agent rule (26, 48, 50, 51, 56). Single vaccination of pregnant ewes with MP-12 results in the protection of both ewes and newborn lambs that receive the colostrum of immunized ewes (50), while the residual virulence of MP-12 induces abortion or fetal malformation in pregnant ewes vaccinated early in gestation (23). The S segment of MP-12 maintains the virulent phenotype (2), and the M and L segments of MP-12 are most likely responsible for MP-12 attenuation (67, 75). It was demonstrated that removal of functional NSs is an effective strategy to attenuate wt RVFV, and the resulting RVFV lacking NSs is an attractive candidate live-attenuated vaccine for Rift Valley fever, e.g., the clone 13 strain, which lacks 69% of the NSs ORFs in the wt RVFV 74HB59 strain backbone (14, 56), or ΔNSs-ΔNSm-rRVFV vaccine, which lacks both NSs and NSm in the wt RVFV ZH501 strain backbone (8). Thus, we generated rMP12-C13type, which encodes strain C13-like NSs in place of MP-12 NSs with the MP-12 backbone, yet mice vaccinated with rMP12-C13type were not completely protected after wt RVFV challenge. To increase the immunogenicity of MP-12, we incorporated the dominant-negative form of PKR into MP-12. rMP12-mPKRN167 encodes a dominant-negative PKR (the N-terminal 167 amino acids of mouse PKR) in place of NSs, which is analogous to human PKRΔE7. PKRΔE7 is alternatively spliced with a deletion of exon 7 and exhibits dominant-negative functions in human cells, but not in mouse cells (39). We confirmed that

rMP12-mPKRN167 inhibits eIF2α phosphorylation in infected MEFs and increases the accumulation of N proteins (Fig. 2).

Mice vaccinated with rMP12-mPKRN167 were completely protected from wt RVFV challenge after a single subcutaneous immunization. MP-12 and rMP12-mPKRN167 induced similar titers of neutralizing antibodies, while some of the mice vaccinated with MP-12 did not raise antibodies at all. All dead mice lacked neutralizing antibodies before wt RVFV challenge, while one mouse vaccinated with rMP12-mPKRN167 survived wt RVFV challenge without neutralizing antibody (Table 1). Thus, neutralizing antibody plays a key role in protection, while some mice may survive wt RVFV challenge without the induction of neutralizing antibodies, as described previously (31).

To understand the significance of PKR degradation for MP-12 immunogenicity, we also made rMP12-NSsR173A, which inhibits host transcription, including IFN-β mRNA synthesis, yet does not degrade PKR. rMP12-NSsR173A poorly accumulated viral proteins at draining lymph nodes and did not induce neutralizing antibodies (data not shown). Thus, it is suggested that PKR degradation is indispensable for the strong immunogenicity of MP-12 and that transcription suppression by NSs inhibits the host immune responses. On the other hand, rMP12-C13type and rMP12-mPKRN167, which lack a host transcription suppression function, were highly immunogenic in mice. Thus, the transcription suppression function is not required for MP-12 immunogenicity, and the suppression of PKR in the absence of host transcription maximizes the efficacy of MP-12 vaccine.

We found that MP-12 does not accumulate viral proteins in the draining lymph nodes, while rMP12-C13type and rMP12-mPKRN167, which lack NSs, could accumulate viral proteins. We further confirmed that viral N proteins were localized in the cytoplasm of CD11c-positive and langerin-negative cells (see Fig. S1 in the supplemental material), which were morphologically identical to DCs (Fig. 6). Recent findings suggested that RVFV lacking NSs can replicate in DCs, macrophages, and granulocytes in IFNAR1-deficient mice (19), and DC-SIGN is one of the receptors of RVFV (42), supporting the notion that DCs are the major target of rMP12-mPKRN167. Our results also suggest that a lack of NSs-mediated host transcription suppression leads to efficient accumulation of infected DCs. It is known that foreign antigens that are administered via the subcutaneous route are trapped by dermal DCs (dDCs) in the dermis, which later migrate into the local draining lymph node, where antigen presentation to B and T cells takes place through dDCs (33). Thus, efficient accumulation of viral proteins in DCs in draining lymph nodes may explain the strong immunogenicity of rMP12-mPKRN167 (Fig. 3C and Table 1).

Because MP-12 did not accumulate in the draining lymph nodes at 1, 2, or 3 days p.i. (Fig. 5), we wondered how MP-12 can induce host immune responses. Cytokines and chemokines, including IL-5, IFN-γ, IL-17, GM-CSF, MIP-1β, RANTES, KC, and eotaxin, were significantly increased in sera of mice that were vaccinated with MP-12 (Fig. 7), while some mice that were vaccinated with MP-12 showed detectable viremia (Fig. 3B). It is likely that MP-12 can induce cytokines secreted by all three T helper cell subsets in a systemic manner. The most susceptible target cells of wt RVFV in mice are hepatocytes (70), while the spleen removes blood-borne pathogens and cell debris from circulation (46). Replication of MP-12 is observed in mouse liver, although the titer is approximately 1,000 times lower than that of wt RVFV (20). Thus, it might be possible that MP-12 reaches the liver or spleen by escaping host immune responses at the draining lymph nodes, while rMP12-C13type or rMP12-mPKRN167 induces a local immune response in the draining lymph nodes.

Based on our study, MP-12 encoding dominant-negative PKR is a highly efficacious vaccine candidate for Rift Valley fever. To develop such a vaccine, we need to address the following issues: (i) host specificity of dominant-negative PKR and (ii) the safety of dominant-negative PKR. It is known that human PKRΔE7 does not exhibit a dominant-negative function in mouse cells (39). On the other hand, PKRΔE7 inhibits PKR of *Chlorocebus aethiops* (Vero E6 cells) (27). The phylogenetic analysis of the PKR gene suggests that ruminant PKRs are distantly related to human or murine PKR (66). Thus, the dominant-negative PKR specific to each host species will need to be evaluated before vaccine development. The safety of dominant-negative PKR should also be addressed. Past studies suggested that increased translation initiation by introducing eIF2α encoding an alanine at serine 51 into spontaneously immortalized NIH 3T3 cells, which are deficient in the INK4 locus (63), supported the development of tumors, while the same study using 3T3 L1 cells that retain the INK4 locus did not lead to tumor formation (60). Similarly, the introduction of dominant-negative PKR, PKRΔ6, which lacks exon 6 of human PKR, into NIH 3T3 cells induced tumor formation (36), while PKR-null mice do not have high frequencies of tumors (1, 76), suggesting that the suppression of PKR is not the sole factor to induce tumors. On the other hand, PKR is often activated in tumors (35, 65), and the apoptosis of cancer cells was triggered by adenovirus encoding PKRΔ6 (58). In this study, we tested the dominant-negative PKR in a live-attenuated vaccine and demonstrated successful improvement of immunogenicity and efficacy. Mice vaccinated with rMP12-mPKRN167 were in good health for at least 180 days after immunization. The mice did not develop viremia after immunization, suggesting rMP12-mPKRN167 virus was rapidly cleared once type I IFNs were induced in response to abundant viral replication in primary infected cells.

In summary, we demonstrated that MP-12 encoding dominant-negative PKR is highly efficacious and applicable to DIVA. It protects all mice from wt RVFV challenge by a single subcutaneous inoculation. The viral antigens were detected in DCs in draining lymph nodes, and vaccinated mice elicited long-term neutralizing antibody response. In contrast, the parental MP-12 strain did not accumulate viral proteins in local draining lymph nodes and stimulated the host immune response in a manner distinct from that of strains lacking NSs. A novel approach using dominant-negative PKR will be useful to increase the efficacy and immunogenicity of vaccine candidates.

ACKNOWLEDGMENTS

We thank R.B. Tesh at UTMB for providing anti-RVFV mouse polyclonal antibody. We also thank Judith Aronson at the UTMB histopathology core for her suggestions on the histopathological approach and the staffs of the animal resource center at UTMB for daily monitoring and care of mice in this study. The study was supported by useful suggestions at monthly meetings organized by the Western Regional Center of Excellence for Biodefense and Emerging Infectious Diseases Research.

This work was supported by grants U54 AI057156 (NIAID, the Western Regional Center of Excellence for Biodefense and Emerging Infectious Diseases Research) and R01 AI08764301-A1 (NIAID) and funding from the Sealy Center for Vaccine Development at UTMB. B.K. was supported by the James W. McLaughlin Fellowship Fund at UTMB.

REFERENCES

1. **Abraham N, et al.** 1999. Characterization of transgenic mice with targeted disruption of the catalytic domain of the double-stranded RNA-dependent protein kinase, PKR. J. Biol. Chem. **274**:5953–5962.
2. **Billecocq A, et al.** 2008. RNA polymerase I-mediated expression of viral RNA for the rescue of infectious virulent and avirulent Rift Valley fever viruses. Virology **378**:377–384.
3. **Billecocq A, et al.** 2004. NSs protein of Rift Valley fever virus blocks interferon production by inhibiting host gene transcription. J. Virol. **78**: 9798–9806.
4. **Bird BH, et al.** 2008. Rift Valley fever virus lacking the NSs and NSm genes is highly attenuated, confers protective immunity from virulent virus challenge, and allows for differential identification of infected and vaccinated animals. J. Virol. **82**:2681–2691.
5. **Bird BH, Albarino CG, Nichol ST.** 2007. Rift Valley fever virus lacking NSm proteins retains high virulence in vivo and may provide a model of human delayed onset neurologic disease. Virology **362**:10–15.
6. **Bird BH, Khristova ML, Rollin PE, Ksiazek TG, Nichol ST.** 2007. Complete genome analysis of 33 ecologically and biologically diverse Rift Valley fever virus strains reveals widespread virus movement and low genetic diversity due to recent common ancestry. J. Virol. **81**:2805–2816.
7. **Bird BH, Ksiazek TG, Nichol ST, Maclachlan NJ.** 2009. Rift Valley fever virus. J. Am. Vet. Med. Assoc. **234**:883–893.
8. **Bird BH, et al.** 2011. Rift Valley fever virus vaccine lacking the NSs and NSm genes is safe, non-teratogenic, and confers protection from viremia, pyrexia, and abortion following lethal challenge in adult and pregnant sheep. J. Virol. **85**:12901–12909.
9. **Borio L, et al.** 2002. Hemorrhagic fever viruses as biological weapons: medical and public health management. JAMA **287**:2391–2405.
10. **Bouloy M, et al.** 2001. Genetic evidence for an interferon-antagonistic function of Rift Valley fever virus nonstructural protein NSs. J. Virol. **75**:1371–1377.
11. **Caplen H, Peters CJ, Bishop DH.** 1985. Mutagen-directed attenuation of Rift Valley fever virus as a method for vaccine development. J. Gen. Virol. **66**:2271–2277.
12. **Carroll SA, et al.** 2011. Genetic evidence for Rift Valley fever outbreaks in Madagascar resulting from virus introductions from the East African mainland rather than enzootic maintenance. J. Virol. **85**:6162–6167.
13. **Daubney R, Hudson JR.** 1931. Enzootic hepatitis or Rift Valley fever: an undescribed virus disease of sheep cattle and man from east Africa. J. Pathol. Bact. **34**:545–579.
14. **Dungu B, et al.** 2010. Evaluation of the efficacy and safety of the Rift Valley Fever Clone 13 vaccine in sheep. Vaccine **28**:4581–4587.
15. **Fukushi S, et al.** 2012. Antigen-capture ELISA for the detection of Rift Valley fever virus nucleoprotein using new monoclonal antibodies. J. Virol. Methods **180**:68–74.
16. **Gale M, Jr, Tan SL, Katze MG.** 2000. Translational control of viral gene expression in eukaryotes. Microbiol. Mol. Biol. Rev. **64**:239–280.
17. **Garcia MA, et al.** 2006. Impact of protein kinase PKR in cell biology: from antiviral to antiproliferative action. Microbiol. Mol. Biol. Rev. **70**:1032–1060.
18. **Giglia-Mari G, et al.** 2004. A new, tenth subunit of TFIIH is responsible for the DNA repair syndrome trichothiodystrophy group A. Nat. Genet. **36**:714–719.
19. **Gommet C, et al.** 2011. Tissue tropism and target cells of NSs-deleted Rift Valley fever virus in live immunodeficient mice. PLoS Negl. Trop. Dis. **5**:e1421. doi:10.1371/journal.pntd.0001421.
20. **Gray KK, et al.** 2012. Chemotactic and inflammatory responses in the liver and brain are associated with pathogenesis of Rift Valley fever virus infection in the mouse. PLoS Negl. Trop. Dis. **6**:e1529. doi:10.1371/journal.pntd.0001529.
21. **Habjan M, et al.** 2009. NSs protein of Rift Valley fever virus induces the specific degradation of the double-stranded RNA-dependent protein kinase. J. Virol. **83**:4365–4375.
22. **Harrell MI, Iritani BM, Ruddell A.** 2008. Lymph node mapping in the mouse. J. Immunol. Methods **332**:170–174.
23. **Hunter P, Erasmus BJ, Vorster JH.** 2002. Teratogenicity of a mutagenised Rift Valley fever virus (MVP 12) in sheep. Onderstepoort J. Vet. Res. **69**:95–98.
24. **Iben S, et al.** 2002. TFIIH plays an essential role in RNA polymerase I transcription. Cell **109**:297–306.
25. **Ikegami T, Makino S.** 2011. The pathogenesis of Rift Valley fever. Viruses **3**:493–519.
26. **Ikegami T, Makino S.** 2009. Rift Valley fever vaccines. Vaccine **27**(Suppl. 4):D69–D72.
27. **Ikegami T, et al.** 2009. Rift Valley fever virus NSs protein promotes post-transcriptional downregulation of protein kinase PKR and inhibits eIF2alpha phosphorylation. PLoS Pathog. **5**:e1000287. doi:10.1371/journal.ppat.1000287.
28. **Ikegami T, et al.** 2003. Immunoglobulin G enzyme-linked immunosorbent assay using truncated nucleoproteins of Reston Ebola virus. Epidemiol. Infect. **130**:533–539.
29. **Ikegami T, Won S, Peters CJ, Makino S.** 2006. Rescue of infectious Rift Valley fever virus entirely from cDNA, analysis of virus lacking the NSs gene, and expression of a foreign gene. J. Virol. **80**:2933–2940.
30. **Ito N, et al.** 2003. Improved recovery of rabies virus from cloned cDNA using a vaccinia virus-free reverse genetics system. Microbiol. Immunol. **47**:613–617.
31. **Jansen van Vuren P, Tiemessen CT, Paweska JT.** 2011. Anti-nucleocapsid protein immune responses counteract pathogenic effects of Rift Valley fever virus infection in mice. PLoS One **6**:e25027. doi:10.1371/journal.pone.0025027.
32. **Kalveram B, Lihoradova O, Ikegami T.** 2011. NSs protein of Rift Valley fever virus promotes post-translational downregulation of the TFIIH subunit p62. J. Virol. **85**:6234–6243.
33. **Kaplan DH.** 2010. Langerhans cells: not your average dendritic cell. Trends Immunol. **31**:437.
34. **Khan F, He M, Taussig MJ.** 2006. Double-hexahistidine tag with high-affinity binding for protein immobilization, purification, and detection on Ni-nitrilotriacetic acid surfaces. Anal. Chem. **78**:3072–3079.
35. **Kim SH, Gunnery S, Choe JK, Mathews MB.** 2002. Neoplastic progression in melanoma and colon cancer is associated with increased expression and activity of the interferon-inducible protein kinase, PKR. Oncogene **21**:8741–8748.
36. **Koromilas AE, Roy S, Barber GN, Katze MG, Sonenberg N.** 1992. Malignant transformation by a mutant of the IFN-inducible dsRNA-dependent protein kinase. Science **257**:1685–1689.
37. **Le May N, et al.** 2004. TFIIH transcription factor, a target for the Rift Valley hemorrhagic fever virus. Cell **116**:541–550.
38. **Le May N, et al.** 2008. A SAP30 complex inhibits IFN-beta expression in Rift Valley fever virus infected cells. PLoS Pathog. **4**:e13. doi:10.1371/journal.ppat.0040013.
39. **Li S, Koromilas AE.** 2001. Dominant negative function by an alternatively spliced form of the interferon-inducible protein kinase PKR. J. Biol. Chem. **276**:13881–13890.
40. **Lihoradova OA, et al.** 2007. The Homingbac baculovirus cloning system: an alternative way to introduce foreign DNA into baculovirus genomes. J. Virol. Methods **140**:59–65.
41. **Linthicum KJ, Davies FG, Kairo A, Bailey CL.** 1985. Rift Valley fever virus (family Bunyaviridae, genus Phlebovirus). Isolations from Diptera collected during an inter-epizootic period in Kenya. J. Hyg. (London) **95**:197–209.
42. **Lozach PY, et al.** 2011. DC-SIGN as a receptor for phleboviruses. Cell Host Microbe **10**:75–88.
43. **Lu H, Zawel L, Fisher L, Egly JM, Reinberg D.** 1992. Human general transcription factor IIH phosphorylates the C-terminal domain of RNA polymerase II. Nature **358**:641–645.
44. **Mandell RB, Flick R.** 2011. Rift Valley fever virus: a real bioterror threat. J. Bioterror. Biodef. **2**:108.
45. **Mandell, R. B., and Flick. R.** 2010. Rift Valley fever virus: an unrecognized emerging threat? Hum. Vaccin. **6**:597–601.
46. **Mebius RE, Kraal G.** 2005. Structure and function of the spleen. Nat. Rev. Immunol. **5**:606–616.
47. **Merad M, Ginhoux F, Collin M.** 2008. Origin, homeostasis and function of Langerhans cells and other langerin-expressing dendritic cells. Nat. Rev. Immunol. **8**:935–947.
48. **Morrill JC, et al.** 1991. Further evaluation of a mutagen-attenuated Rift Valley fever vaccine in sheep. Vaccine **9**:35–41.
49. **Morrill JC, et al.** 2010. Rapid accumulation of virulent Rift Valley fever virus in mice from an attenuated virus carrying a single nucleotide substitution in the mRNA. PLoS One **5**:e9986. doi:10.1371/journal.pone.0009986.
50. **Morrill JC, et al.** 1987. Pathogenicity and immunogenicity of a mutagen-

attenuated Rift Valley fever virus immunogen in pregnant ewes. Am. J. Vet. Res. **48**:1042–1047.
51. **Morrill JC, Mebus CA, Peters CJ.** 1997. Safety and efficacy of a mutagen-attenuated Rift Valley fever virus vaccine in cattle. Am. J. Vet. Res. **58**: 1104–1109.
52. **Morrill JC, Mebus CA, Peters CJ.** 1997. Safety of a mutagen-attenuated Rift Valley fever virus vaccine in fetal and neonatal bovids. Am. J. Vet. Res. **58**:1110–1114.
53. **Morrill JC, Peters CJ.** 2011. Mucosal immunization of rhesus macaques with Rift Valley fever MP-12 vaccine. J. Infect. Dis. **204**:617–625.
54. **Morrill JC, Peters CJ.** 2003. Pathogenicity and neurovirulence of a mutagen-attenuated Rift Valley fever vaccine in rhesus monkeys. Vaccine **21**:2994–3002.
55. **Morrill JC, Peters CJ.** 2011. Protection of MP-12-vaccinated rhesus macaques against parenteral and aerosol challenge with virulent Rift Valley fever virus. J. Infect. Dis. **204**:229–236.
56. **Muller R, et al.** 1995. Characterization of clone 13, a naturally attenuated avirulent isolate of Rift Valley fever virus, which is altered in the small segment. Am. J. Trop. Med. Hyg. **53**:405–411.
57. **Ogay ID, et al.** 2006. Transfection of insect cell lines using polyethylenimine. Cytotechnology **51**:89–98.
58. **Pataer A, Swisher SG, Roth JA, Logothetis CJ, Corn PG.** 2009. Inhibition of RNA-dependent protein kinase (PKR) leads to cancer cell death and increases chemosensitivity. Cancer Biol. Ther. **8**:245–252.
59. **Pepin M, Bouloy M, Bird BH, Kemp A, Paweska J.** 2010. Rift Valley fever virus (Bunyaviridae: Phlebovirus): an update on pathogenesis, molecular epidemiology, vectors, diagnostics and prevention. Vet. Res. **41**:61.
60. **Perkins DJ, Barber GN.** 2004. Defects in translational regulation mediated by the alpha subunit of eukaryotic initiation factor 2 inhibit antiviral activity and facilitate the malignant transformation of human fibroblasts. Mol. Cell. Biol. **24**:2025–2040.
61. **Peters CJ, Meegan JM.** 1981. Rift Valley fever, p 403–420. *In* Handbook series of zoonoses B: viral zoonoses, vol 1. CRC Press, Boca Raton, FL.
62. **Pittman PR, et al.** 1999. Immunogenicity of an inactivated Rift Valley fever vaccine in humans: a 12-year experience. Vaccine **18**:181–189.
63. **Quelle DE, et al.** 1995. Cloning and characterization of murine p16INK4a and p15INK4b genes. Oncogene **11**:635–645.
64. **Randall R, Gibbs CJ, Jr, Aulisio CG, Binn LN, Harrison VR.** 1962. The development of a formalin-killed Rift Valley fever virus vaccine for use in man. J. Immunol. **89**:660–671.
65. **Roh MS, et al.** 2005. Expression of double-stranded RNA-activated protein kinase in small-size peripheral adenocarcinoma of the lung. Pathol. Int. **55**:688–693.
66. **Rothenburg S, Deigendesch N, Dey M, Dever TE, Tazi L.** 2008. Double-stranded RNA-activated protein kinase PKR of fishes and amphibians: varying the number of double-stranded RNA binding domains and lineage-specific duplications. BMC Biol. **6**:12.
67. **Saluzzo JF, Smith JF.** 1990. Use of reassortant viruses to map attenuating and temperature-sensitive mutations of the Rift Valley fever virus MP-12 vaccine. Vaccine **8**:369–375.
68. **Schmaljohn C, Nichol ST.** 2007. Bunyaviridae, p 1741–1789. *In* Knipe DM, et al (ed), Fields virology, 5th ed. Lippincott, Williams & Wilkins, Philadelphia, PA.
69. **Schultz P, et al.** 2000. Molecular structure of human TFIIH. Cell **102**: 599–607.
70. **Smith DR, et al.** 2010. The pathogenesis of Rift Valley fever virus in the mouse model. Virology **407**:256–267.
71. **Swanepoel R, Coetzer JAW.** 2004. Rift Valley fever, p 1037–1070. *In* Coetzer JAW, et al. Infectious diseases of livestock with special reference to southern Africa, 2nd ed. Oxford University Press, Cape Town, South Africa.
72. **Turell MJ, et al.** 2008. Potential for North American mosquitoes to transmit Rift Valley fever virus. J. Am. Mosq. Control Assoc. **24**:502–507.
73. **Turell MJ, Faran ME, Cornet M, Bailey CL.** 1988. Vector competence of Senegalese Aedes fowleri (Diptera: Culicidae) for Rift Valley fever virus. J. Med. Entomol. **25**:262–266.
74. **Vialat P, Billecocq A, Kohl A, Bouloy M.** 2000. The S segment of rift valley fever phlebovirus (Bunyaviridae) carries determinants for attenuation and virulence in mice. J. Virol. **74**:1538–1543.
75. **Vialat P, Muller R, Vu TH, Prehaud C, Bouloy M.** 1997. Mapping of the mutations present in the genome of the Rift Valley fever virus attenuated MP12 strain and their putative role in attenuation. Virus Res. **52**:43–50.
76. **Yang YL, et al.** 1995. Deficient signaling in mice devoid of double-stranded RNA-dependent protein kinase. EMBO J. **14**:6095–6106.